Hydrol. Earth Syst. Sci. Discuss., 11, 5747–5791, 2014
www.hydrol-earth-syst-sci-discuss.net/11/5747/2014/
doi:10.5194/hessd-11-5747-2014

Hydrology and Earth System Sciences Discussions

Open Access

Model study of the impacts of future climate change on the hydrology of Ganges–Brahmaputra–Meghna (GBM) basin

M. Masood[1,2], **P. J.-F. Yeh**[3], **N. Hanasaki**[4], **and K. Takeuchi**[1]

[1]International Centre for Water Hazard and Risk Management (ICHARM), PWRI, Tsukuba, Japan
[2]National Graduate Institute for Policy Studies (GRIPS), Tokyo, Japan
[3]National University of Singapore, Singapore 119077, Singapore
[4]National Institute for Environmental Studies, Tsukuba, Japan

Received: 19 April 2014 – Accepted: 3 May 2014 – Published: 2 June 2014

Correspondence to: M. Masood (masood35bd@yahoo.com)

Published by Copernicus Publications on behalf of the European Geosciences Union.

Abstract

The intensity, duration, and geographic extent of floods in Bangladesh mostly depend on the combined influences of three river systems, Ganges, Brahmaputra and Meghna (GBM). In addition, climate change is likely to have significant effects on the hydrology and water resources of the GBM basins and might ultimately lead to more serious floods in Bangladesh. However, the assessment of climate change impacts on basin-scale hydrology by using well-constrained hydrologic modelling has rarely been conducted for GBM basins due to the lack of data for model calibration and validation. In this study, a macro-scale hydrologic model H08 has been applied regionally over the basin at a relatively fine grid resolution (10 km) by integrating the fine-resolution (~ 0.5 km) DEM data for accurate river networks delineation. The model has been calibrated via analyzing model parameter sensitivity and validated based on a long-term observed daily streamflow data. The impact of climate change on not only the runoff, but also the basin-scale hydrology including evapotranspiration, soil moisture and net radiation have been assessed in this study through three time-slice experiments; present-day (1979–2003), near-future (2015–2039) and far-future (2075–2099) periods. Results shows that, by the end of 21st century (a) the entire GBM basin is projected to be warmed by ~ 3 °C (b) the changes of mean precipitation are projected to be +14.0, +10.4, and +15.2 %, and the changes of mean runoff to be +14, +15, and +18 % in the Brahmaputra, Ganges and Meghna basin respectively (c) evapotranspiration is predicted to increase significantly for the entire GBM basins (Brahmaputra: +14.4 %, Ganges: +9.4 %, Meghna: +8.8 %) due to increased net radiation (Brahmaputra: +6 %, Ganges: +5.9 %, Meghna: +3.3 %) as well as warmer air temperature. Changes of hydrologic variables will be larger in dry season (November–April) than that in wet season (May–October). Amongst three basins, Meghna shows the largest hydrological response which indicates higher possibility of flood occurrence in this basin. The uncertainty due to the specification of key model parameters in predicting hydrologic quantities, has also been analysed explicitly in this

HESSD

11, 5747–5791, 2014

study and found that the uncertainty in estimation of runoff, evapotranspiration and net radiation is relatively less. However, the uncertainty in estimation of soil moisture is quite large (coefficient of variation ranges from 11 to 33 % for three basins). It is significant in land use management, agriculture in particular and highlights the necessity of physical observation of soil moisture.

1 Introduction

Bangladesh is situated in the active delta of the world's three major rivers, the Ganges, Brahmaputra and Meghna. The occurrence of water-induced disasters is a regular phenomenon in Bangladesh. Reducing the magnitude of the damage by floods to life and property and minimizing environmental impacts have been the major concerns of disaster management activities in Bangladesh. Due to the complex nature of river systems and their hydrologic and hydraulic characteristics, the tasks of predicting the propagation of floods and the planning of effective mitigation measures are quite difficult. However, the intensity, duration, and geographic extent of floods in Bangladesh mostly depend on the combined influences of these three river systems. Previous studies revealed that flood damages have become more severe and devastating when more than one flood peaks in these three river basins coincide (Mirza, 2003; Chowdhury, 2000).

The Ganges–Brahmaputra–Meghna (hereafter referred to as GBM) river basin with a total area of about 1.7 million km^2 (FAO-AQUASTAT, 2014; Islam et al., 2010) encompasses a number of countries including China, India, Nepal, Bhutan and Bangladesh. This river system is the third largest freshwater outlet in the world to the oceans (Chowdhury and Ward, 2004). During the extreme floods, over 138 700 $m^3 s^{-1}$ of water flows into the Bay of Bengal through a single outlet, which is the largest intensity in the world even exceeding that of the Amazon discharge into the sea by about 1.5 times (FAO-AQUASTAT, 2014). The GBM river basin is unique in the world in terms of diversified climate. For example, the Ganges river basin is characterized

HESSD
11, 5747–5791, 2014

by low precipitation (760–1020 mm year^{-1}) in the northwest upper region and high precipitation (1520–2540 mm year^{-1}) along the coastal areas. High precipitation zones and dry rain shadow areas are located in the Brahmaputra river basin, whereas the world's highest precipitation ($\sim$ 5690 mm year^{-1}) area is situated in the Meghna river basin (FAO-AQUASTAT, 2014).

Several studies have focused on the rainfall and discharge relationships in the GBM basin by (1) identifying and linking the correlation between basin-scale discharge and the El Nino-southern oscillation (ENSO) and sea surface temperature (SST) (Chowdhury and Ward, 2004; Mirza et al., 1998; Nishat and Faisal, 2000), (2) analysing available observed or reanalysis data (Chowdhury and Ward, 2004, 2007; Mirza et al., 1998; Kamal-Heikman et al., 2007), and (3) evaluating historical data of flood events (Mirza, 2003; Islam et al., 2010). Various statistical approaches were used in most of these studies instead of conducting hydrologic model simulations. In recent years, a number of global hydrologic model studies (Haddeland et al., 2011, 2012; Pokhrel et al., 2012) have been conducted. Although their modelling domains include the GBM basin, these global-scale simulations are not well constrained due to the lack of calibration data at the basin scale.

Few studies have been conducted to investigate the impact of climate change on the hydrology and water resources in the GBM basins (Immerzeel, 2008; Kamal et al., 2013; Biemans et al., 2013; Gain et al., 2011; Ghosh and Dutta, 2012; Mirza and Ahmad, 2005a). In most of these studies, future streamflow is predicted on the basis of linear regression between rainfall and streamflow derived from historical data (Immerzeel, 2008; Chowdhury and Ward, 2004; Mirza et al., 2003). Immerzeel (2008) used the multiple regression technique to predict streamflow at the Bahadurabad station (the outlet of Brahmaputra basin) under future temperature and precipitation conditions based on the statistically downscaled GCM output. However, since most of the hydrologic processes are nonlinear, they cannot be predicted accurately by using empirical regression equations derived from historical data and then extrapolating to the future conditions with non-stationary changes. The alternative for the assessment of climate change impacts on basin-scale hydrology is by using well-constrained hydrologic modelling, but this has rarely been conducted for the GBM basin due to the lack of data for model calibration and validation. Ghosh and Dutta (2012) applied a physically-based, macro-scale distributed hydrologic model to study the change of future flood characteristics at the Brahmaputra basin, but their study domain only focused on the regions inside India rather than the entire basin. Gain et al. (2011) estimated future trends in low and high flows in the lower Brahmaputra basin using outputs from a global hydrologic model forced by multiple GCM outputs (grid resolution: 0.5°). Instead of calibrating the model, the simulated future streamflow was weighted against the observations to assess the impact due to climate change. In contrast to the above studies, this study, a hydrologic model simulation will be calibrated and validated based on a long-term (1980–2001) observed daily streamflow data in the GBM basin provided by the Bangladesh Water Development Board (BWDB). It is believed that the availability of this unique long-term streamflow data can lead to more precise estimation of model parameters and hence more accurate simulation of hydrological processes as well as more reliable future projection of the hydrology over the GBM basin.

The objective of this study is to (1) understand the hydro-climatic characteristic of the GBM basin, and to (2) study the impact of future climate changes on the basin-scale hydrology of this basin. A global-scale hydrologic model H08 (Hanasaki et al., 2008, 2014) is applied regionally over the GBM basin at a relatively fine grid resolution (10 km) by integrating the fine-resolution (∼ 0.5 km) DEM data for accurate river networks delineation. The hourly dataset from the Water and Global Change (WATCH) model-inter-comparison project (Weedon et al., 2011) (hereafter referred to as WFD, WATCH Forcing Dataset) is used as the climate forcing data for the historical simulation in this study. WFD is considered as one of the best available global forcing dataset to provide accurate representation of real meteorological events, synoptic activity, seasonal cycles and climate trends (Weedon et al., 2011). The studies by Lucas-Picher et al. (2011) and Siderius et al. (2013) found that for the South Asia and the Ganges respectively, the WFD rainfall is consistent with the observed APHRODITE

HESSD
11, 5747–5791, 2014

data (Yatagai et al., 2012), a gridded (0.25°) rainfall product for the South Asia region developed based on a large number of rain gauge data. For the future simulations, the high-resolution (20 km) forcing data obtained from the Meteorological Research Institute Atmospheric General Circulation Model (MRI-AGCM3.2S) (Mizuta et al., 2012) of the Japan Meteorological Agency (JMA) is used. Small-scale phenomena can be realistically simulated by the high-resolution climatic data while keeping the same quality of the global-scale climate representation as that of the lower-resolution models (Mizuta et al., 2012). Accordingly, the future climate simulations provide a substantial amount of information including possible changes in tropical cyclones, the East Asian monsoon, extreme events as well as various issues related to local and regional climate change. In order to be consistent with the historical data, a simple correction factor (i.e. the ratio between the basin-scale long-term mean precipitation of the WFD data and that of the MRI data) for each basin is applied to the MRI-AGCM3.2S precipitation forcing data. Several time-slice experiments are performed for the present-day (1979–2003), near-future (2015–2039) and far-future (2075–2099) periods.

This modelling study makes advances from previous studies in four aspects. First, a hydrologic model H08 (Hanasaki et al., 2008) is used which has been demonstrated suitable for large scale analyses. The model is calibrated for the GBM basin via analysing model parameter sensitivity by Monte Carlo simulation. The model has been validated against daily observed streamflow satisfactorily. Moreover, the uncertainty due to the determination of key model parameters in predicting hydrologic quantities is analysed explicitly here. Second, three large basins GBM and their spatial variability are analysed in this study which benefit the analysis of their combined influences on the large-scale hydrologic floods and droughts occurred in Bangladesh as reported extensively in literature (Chowdhury, 2000; Mirza, 2003). Third, the impact of climate change on not only the discharge but also the basin-scale hydrology including evapotranspiration, soil moisture and net radiation is assessed in this study, whereas in most previous work the climate change impact on streamflow only was the single main focus. Finally, the AGCM data are employed in this study which have higher

HESSD
11, 5747–5791, 2014

horizontal resolution (20 km) than any other data used in previous studies. This could in principle allow AGCM to simulate the phenomena closely related to local topography and wind distributions more realistically, and hence to provide better future projection (Endo et al., 2012).

The paper is organized into five sections as follows. A brief description of the data and hydrologic model used is presented in Sect. 2. Section 3 presents the methodology of model setup as well as the results from model parameter sensitivity analysis. Results and discussion are presented in Sect. 4. Finally, conclusions are drawn.

2 Data and tools

2.1 Meteorological forcing datasets

The WATCH Forcing Data set (WFD) (Weedon et al., 2011) are used to drive the H08 model for the historical simulation. The WFD variables, including rainfall, snowfall, surface pressure, air temperature, specific humidity, wind speed, long-wave downward radiation, and shortwave downward radiation were taken from the ERA-40 reanalysis product of the European Centre for Medium Range Weather Forecasting (ECMWF). The one-degree resolution ERA40 reanalysis data were interpolated into the half-degree resolution on the Climate Research Unit of the University of East Anglia (CRU) land mask, adjusted for elevation changes where needed and bias-corrected using monthly observations. For detailed information on the WFD, see Weedon et al. (2011) and Weedon et al. (2010). The albedo values are based on the monthly albedo data form the Second Global Soil Wetness Project (GSWP2).

2.2 Hydrologic data

Observed river water level and discharge data from 1980 to 2012 for the hydrological stations located inside the Bangladesh were provided by the Hydrology Division, Bangladesh Water Development Board (BWDB). The data were mainly from the

HESSD
11, 5747–5791, 2014

outlets of three basins, i.e. the Ganges basin at Hardinge Bridge, the Brahmaputra basin at Bahadurabad, and the Meghna basin at Bhairab Bazar (Fig. 1). River water levels were regularly measured 5 times (at 6 a.m., 9 a.m., 12 p.m., 3 p.m., and 6 p.m.) a day and discharges were measured weekly by the velocity-area method. Since the Brahmaputra river is highly braided, the discharge measurement at Bahadurabad was carried out on multiple channels. In contrast, the Meghna river at Bhairab Bazar is seasonally tidal – after withdrawal of the monsoon the river at this station becomes tidal, and from December to May the river shows both a horizontal and a vertical tide (Chowdhury and Ward, 2004). Under this condition, during the dry season, tidal discharge measurements were made at this station once per month. Daily discharges of Ganges and Brahmaputra were calculated from the daily water level data by using the rating equations developed by the Institute of Water Modelling (IWM) (IWM, 2006). Rating equation for the Meghna river was not reported in literature. In this study an attempt was made to develop the rating equation for the Meghna basin.

2.3 Topographic data

DEM data were collected from the HydroSHEDS (Hydrological data and maps based on SHuttle Elevation Derivatives at multiple Scales) (HydroSHEDS, 2014). It offers a suite of geo-referenced data sets (vector and raster), including stream networks, watershed boundaries, drainage directions, and ancillary data layers such as flow accumulations, distances and river topology information (Lehner et al., 2006). The HydroSHEDS data were derived from elevation data of the Shuttle Radar Topography Mission (SRTM) at ~ 0.5 km resolution. Preliminary quality assessments indicate that the accuracy of HydroSHEDS significantly exceeds that of existing global watershed and river maps (Lehner et al., 2006).

HESSD
11, 5747–5791, 2014

2.4 AGCM data: MRI-AGCM3.2S

MRI-AGCM3.2S (where the "S" refers to the "super-high resolution") (Mizuta et al., 2012) has been used for future simulation. MRI-AGCM3.2S is based on an atmospheric climate model with a 20 km grid model developed jointly by Meteorological Research Institute (MRI) and Japan Meteorological Agency (JMA). The model provided information on possible climate change induced by global warming, including future changes in tropical cyclones, the East Asian monsoon, extreme events, and blockings. MRI-AGCM3.2S is revised version from the previous MRI-AGCM3.1, with many new developments of parameterization schemes for various physical processes (Mizuta et al., 2012). The model shows improvements in simulating heavy monthly-mean precipitation, global distribution of tropical cyclones, and the seasonal march of East Asian summer monsoon. Improvements in the model simulated climatologies have been confirmed (Mizuta et al., 2012). Climate change impacts on the south Asian climate were assessed in several recent studies by using the MRI-AGCM3.2S dataset (Rahman et al., 2012; Endo et al., 2012; Kwak et al., 2012). However, Rahman et al. (2012) found that although the MRI-AGCM3.2S can reproduce precipitation reasonably well in the pre-monsoon, post-monsoon and dry periods (winter), it under-simulated the precipitation during the monsoon season over Bangladesh. The bias corrected (method proposed by Inomata et al., 2011) precipitation data has been checked with WFD data over GBM basin and found as slightly underestimated as well. Therefore, the bias of MRI-AGCM3.2S's precipitation dataset has been corrected by multiplying a correction coefficient (ratio between basin averaged long term yearly mean precipitation from WFD and that from MRI) for each GBM basins.

2.5 Hydrologic model: H08

H08 is a macro-scale hydrological model developed by Hanasaki and others (Hanasaki et al., 2008) which consists of six main modules: land surface hydrology, river routing, crop growth, reservoir operation, environmental flow requirement estimation,

HESSD
11, 5747–5791, 2014

and anthropogenic water withdrawal. For this study, only two modules, land surface hydrology and river routing are used. The land surface hydrology module calculates the energy and water budget, on the land surface as forced by high temporal-resolution meteorological data.

The runoff scheme in H08 is based on the bucket model concept (Manabe, 1969), but differs from the original formulation in certain important aspects. Although runoff is generated only when the bucket is overfilled in the original bucket model, H08 uses a "leaky bucket" formulation of which subsurface runoff occurs continually as a function of soil moisture. Soil moisture is expressed as a single-layer bucket which is 15 cm deep for all soil and vegetation types. When the bucket is empty, soil moisture is at the wilting point; when the bucket is full, soil moisture is at field capacity. Evapotranspiration is expressed as a function of potential evapotranspiration and soil moisture (Eq. 2). Potential evapotranspiration and snowmelt are calculated from the surface energy balance (Hanasaki et al., 2008).

Potential evaporation E_P is expressed in this model as

$$E_P(T_S) = \rho C_D U (q_{SAT}(T_S) - q_a), \tag{1}$$

where ρ is the density of air, C_D is the bulk transfer coefficient, U is the wind speed, $q_{SAT}(T_S)$ is the saturated specific humidity at surface temperature, and q_a is the specific humidity. Evaporation from a surface (E) is expressed as

$$E = \beta E_P(T_S) \tag{2}$$

where

$$\beta = \begin{cases} 1 & 0.75 W_f \leq W \\ W/W_f & W < 0.75 W_f \end{cases} \tag{3}$$

where W is the soil water content and W_f is the soil water content at field capacity (fixed at $150\,\mathrm{kg\,m^{-2}}$).

HESSD
11, 5747–5791, 2014

Surface runoff (Q_s) is generated whenever the soil water content exceeds the field capacity:

$$Q_s = \begin{cases} W - W_f & W_f < W \\ 0 & W \le W_f \end{cases} \tag{4}$$

Subsurface runoff (Q_{sb}) is incorporated to the model as

$$Q_{sb} = \frac{W_f}{\tau} \left(\frac{W}{W_f} \right)^{\gamma}, \tag{5}$$

where τ is a time constant and γ is a parameter characterizing the degree of nonlinearity of Q_{sb}. These two parameters have been calibrated in this study which is described in Sect. 3.1.

The river module is identical to the Total Runoff Integrating Pathways (TRIP) model (Oki and Sud, 1998). The module has a digital river map which covers the whole globe at a spatial resolution of 1° (~ 111 km). The land–sea mask is identical to the GSWP2 meteorological forcing input and a flow velocity fixed at 0.5 m s^{-1}. However a new digital river map of GBM basin with a spatial resolution of ~ 10 km has been prepared for this study. The module accumulates runoff generated by the land surface model and rout them downstream to become streamflow.

3 Methodology: model setup and simulation

Figure 2 presents the methodology used in this study from model setup to the historical and future simulations. H08 model has been setup to simulate at ~ 10 km (5 min) resolution. The model is calibrated to find the best parameter sets through parameter sensitivity study by Monte Carlo simulation technique, and validated with observed daily streamflow data.

The default river module of H08 uses the digital river map from the Total Runoff Integrating Pathways model (TRIP) (Oki and Sud, 1998) with a global resolution of 1° (111 km). However, this resolution is too course for the regional simulation in this study in which the spatial resolution of 10 km is used. Therefore, a digital river map of same resolution has been prepared with integrating finer (∼ 0.5 km) DEM data.

3.1 Parameter sensitivity

A Monte Carlo simulation is conducted to investigate the sensitivity of H08 model parameters to simulation results. The most sensitive parameters in H08 include the root-zone depth d [m], bulk transfer coefficient C_D [–] controlling the potential evaporation (Eq. 1), and the parameters controlling subsurface flow, namely, τ [day] and γ [–] (Eq. 5) (Hanasaki et al., 2014), hence they are treated as calibration parameters in this study. The parameter τ is a time constant that sets the daily maximum subsurface runoff. The parameter γ is a shape parameter that sets the relationship between subsurface flow and soil moisture (Hanasaki et al., 2008). The default values of these sensitive parameters are 1 m for d, 0.003 for C_D, 100 days for τ, and 2 for γ. For each of the four parameters, five values are selected from their feasible ranges. The Monte Carlo simulation of H08 model were run by using all the combinations of four parameters, which consists of a total of 5^4 (= 625) simulations. The simulation and calibration were conducted using an 11 year (1980–1990) atmospheric forcing data.

Figure 3 plots the 11 year climatology of simulated total runoff, surface runoff and sub-surface runoff of Brahmaputra basin. Each of the five lines in each panel represents the average of 5^3 (= 125) runs with one of the 4 calibration parameters fixed at a given value. It shows the overall sensitivity of selected model parameters to flow partitioning and evaporation simulation. When d is low, surface runoff is high (due to the higher saturated fractional area) (Fig. 3b). As d increases, sub-surface runoff increases and surface runoff decreases (Fig. 3c and b). Due to these compensating effects, the effect of d on the total runoff becomes more complex: from March to August, a higher

HESSD
11, 5747–5791, 2014

d causes a lower total runoff, but the trend reverses from August on for Brahmaputra river basin. Similar behaviour is observed for other two basins (figure not shown).

The parameter C_D is the bulk transfer coefficient to calculate potential evaporation (Eq. 1); so its effect on runoff is small (Fig. 3d–f). However, a higher C_D gives a lower runoff (both surface and sub-surface) as a high C_D causes more evaporation (Eqs. 1 and 2) and less runoff. The effect of parameter γ on runoff is also less relative to d and τ. As γ increases, surface runoff increases and sub-surface runoff decreases (Fig. 3h and i). The effect of γ on the total runoff becomes negligible due to the compensating effects (Fig. 3g).

As shown in Eq. (5) and Fig. 3k and l, the parameter τ has a major impact to surface and sub-surface flow partitioning. A larger τ corresponds to larger surface runoff and hence smaller sub-surface runoff (Fig. 3k and l). The parameter τ, despite its significant impact on both surface and sub-surface runoff, has relatively small impact on total runoff (Fig. 3j).

Figure 4 shows the 11 year average annual total runoff, surface runoff and sub-surface runoff. Each curve represents the average of the 125 runs in which only one of the four parameters were fixed. As seen from Fig. 4a, although the amount of total runoff is insensitive to d, the partitioning between surface runoff and sub-surface is remarkably sensitive to d suggesting the equifinality in the optimal parameter set: i.e., an optimal parameter set calibrated against observed streamflow does not necessarily lead to a unique optimal flow partitioning. It also implies that if only one criterion is used in the parameter calibration, then model simulations for other hydrologic variables may not be constrained. Moreover, other than d, the parameter τ also has a significant impact on the flow partitioning (Fig. 4d). In contrast, the other two parameters have almost no impacts on flow partitioning (Fig. 4b and c). As expected, C_D and γ have more impacts on sub-surface runoff than surface runoff (Fig. 4b, c, f, g, j and k). Sub-surface runoff decreases as these two parameters increase whereas surface runoff remains relatively unchanged.

HESSD
11, 5747–5791, 2014

These four calibration parameters have the combined influences on total runoff partitioning as well as simulations of other hydrologic variables. To summarize, (1) the effect of d on the total runoff is complex: the trend is reversed between the two halves of a year; (2) parameters d and τ have a significant impact on flow partitioning whereas C_D and γ have less impact on runoff simulation; (3) the impact of d and τ is reversed between surface and sub-surface runoff: surface runoff increases as d decreases and τ increases.

Figure 5 plots the envelopes of the simulated discharges by using 10 optimal parameter combinations according to Nash–Sutcliffe coefficient of efficiency (NSE) (Nash and Sutcliffe, 1970) for the Brahmaputra and Ganges basin. It is observed that the spread of envelopes is located mainly in the low flow period (dry season from November to March) in Brahmaputra basin (Fig. 5a). No surface runoff generated in dry season when soil moisture content is less than the field capacity (Eq. 4 and Fig. 3b). It is noted that among the 10 optimal parameter combinations τ is 150, C_D is 0.001, d and γ ranges from 2 to 3 and 1.0 to 1.5 respectively. The spread of envelopes is mainly due to the variation of the d and γ values. As d increases, the sub-surface runoff increases (Figs. 3c and 4a). On the other hand, in the case of Ganges basin the spread of envelopes is observed through the entire period of a year (in low flow as well as in peak flow regimes) (Fig. 5b). Among the 10 optimal parameter combinations it is found that parameter C_D is 0.008, τ is 150, γ is 4, and d ranges from 3 to 4. In dry period when surface runoff is zero sub-surface runoff increases as d increases. A higher C_D causes higher evaporation which influences runoff as well (Eq. 1). As discussed earlier, the effect of d on the total runoff is complex which results in the variation of simulated runoff throughout the year. The spread of envelopes is large in the peak flow period as the sensitivity of both surface and sub-surface runoff is also large with respect to the value of d (not shown in figure).

HESSD
11, 5747–5791, 2014

3.2 Calibration and validation

The historical simulation from 1980 to 2001 is divided into two periods, with the first half (1980–1990) selected as the calibration period and the second half (1991–2001) for validation. Model performance is evaluated by comparing observed and simulated daily streamflow using the Nash–Sutcliffe efficiency (NSE) (Nash and Sutcliffe, 1970), the optimal objective function for assessing the overall fit of a hydrograph (Sevat and Dezetter, 1991). A (series of) sensitivity analysis of H08 parameters was conducted by using the Monte Carlo simulation from which the best 10 sets of parameter combinations are determined as discussed in previous section. These 10 sets of optimal parameter will be used to quantify the uncertainty due to model parameters in subsequent historical and future simulations. Figure 6 plots the daily hydrographs at the outlets of three river basins in comparison with the corresponding daily flow observations for both calibration and validation periods. The obtained NSE for the calibration (validation) period is 0.80 (0.76), 0.45 (0.43), and 0.70 (0.82) and correlation coefficient is 0.90 (0.88), 0.71 (0.73) and 0.88 (0.91) for the Brahmaputra, Ganges, and Meghna River basins, respectively. The overall fit of the hydrographs in the Brahmaputra and Meghna basins are satisfactory while the simulated hydrograph in Ganges shows a time lag of about a week through the entire period (1980–2001). Relatively poor simulation in the Ganges basin is likely due to the large amount of upstream water use (FAO-AQUASTAT, 2014; Nishat and Rahman, 2009) which was not accounted for in current model simulations. Simulated discharge at the outlet of the Meghna basin overestimates the peak discharge, although the overall fit is satisfactory. This is likely due to that the Meghna as a tidal river may have the reduced discharge caused by the backwater effect during the high flow period. However, the backwater effect is not considered in the present model simulation.

4 Result and discussion

H08 has been calibrated and validated forced by WFD forcing data and MRI-AGCM3.2S to simulate in three time-slice, present (1979–2003), near-future (2015–2039) and the far-future (2075–2099). Simulation results for future periods have been then compared with that of present period (1979–2003) forced by MRI-AGCM3.2S to assess the effect of climate change on the hydrology and water resources of GBM in terms of precipitation, air temperature, evapotranspiration, soil moisture and net radiation by graphical and statistical methods.

4.1 Seasonal cycle

Table 2 and Fig. 7 plots the 22 year (1980–2001) mean seasonal cycles of the climatic (from WFD forcing) and hydrological (from calibrated hydrologic model simulation) quantities averaged over these three basins. The interannual variation of precipitation in Brahmaputra and Meghna was mainly from May to September (Fig. 7a and c) whereas for Ganges was from June to October. However, magnitude differed substantially. Meghna had its maximum precipitation in May with 32 mm day^{-1} whereas Brahmaputra and Ganges had in July with 15 and 13 mm day^{-1} respectively. The seasonal variation of runoff of all basins corresponded well with that of precipitation. Runoff (Fig. 7j–l) in Ganges was much less (maximum annual mean was 4 mm day^{-1} in August) compared to other two basins (Brahmaputra: 9.5 mm day^{-1}, Meghna: 15 mm day^{-1}). ET of Brahmaputra was quite low (mean annual total was 252 mm) compared to other two basins (Ganges: 772 mm, Meghna: 703 mm). Lower ET of Brahmaputra might be due to having less vegetated area (basin-averaged Normalized Difference Vegetation Index (NDVI) of Brahmaputra is 0.38 whereas for Ganges and Meghna, NDVI are 0.41 and 0.65 respectively, NEO, 2014) and cooler air temperature in this basin compared to other two basins. However, the pattern of seasonal variation of ET in Brahmaputra and in Meghna was quite similar except a drop in July for Brahmaputra (Fig. 7m and o). ET was pretty stable from May to October in Brahmaputra and Meghna while Ganges

HESSD
11, 5747–5791, 2014

had a high peak in September with interannual average of 4.1 mm day^{-1}. The pattern as well as magnitude of seasonal variation of soil moisture was quite different in these basins (Fig. 7p–r). However, peak of interannual average of soil moisture reached in August in all three basins.

Figure 7d–f present the seasonal cycle of basin average air temperature (Tair). Brahmaputra was much cooler (mean temperature was 9.1 °C) than that of other two basins (Ganges: 21.7 °C and Meghna: 23.0 °C). Figure 7g–i plot the 22 year mean seasonal cycles of net radiation averaged over these three basins. The pattern of seasonal variation of net radiation was similar though magnitudes were bit different among these basins. The maximum net radiation of Brahmaputra, Ganges and Meghna were about 49; 114 and 102 W m^{-2} while mean net radiations were about 30; 74 and 78 W m^{-2} respectively (Table 2).

4.2 Correlation between meteorological and hydrological variables

Figure 8 presents the correlation between monthly mean of meteorological variables and that of hydrological variables of three river basins. Three different color representing data of three different seasons; dry/winter (November–March), pre-monsoon (April–June) and monsoon (July–October). Distinct relationship between hydrological and meteorological variables in three different seasons has been observed from the figure.

Total runoff and surface runoff of Brahmaputra have stronger correlation (correlation coefficient (cc) are 0.95 and 0.97 respectively) with precipitation than that of other two basins. However, sub-surface runoff of Brahmaputra has weaker correlation (cc = 0.62) with precipitation than that of Ganges (cc = 0.72) and Meghna (cc = 0.80). These relationships imply that the deeper soil depth enhances correlation-ship between sun-surface runoff and precipitation. Meghna, having deeper root zone depth (calibrated $d = 5$ m), generate larger amount of sub-surface runoff (83 % of total runoff) than other two basins, which result stronger relationship with precipitation. Consequently, soil moisture of Meghna also shows stronger correlation (cc = 0.93) with precipitation than that of Brahmaputra (cc = 0.77) and of Ganges (cc = 0.80). Actually, this is quite reasonable since deeper soil depth buffers short-term variation in soil moisture and enhances relationship between precipitation and long-term mean soil moisture.

The relationship of the evapotranspiration process with various atmospheric conditions, such as radiation, air temperature, and water availability, is quite complex (Shaaban et al., 2011). Moreover, different methods for estimating potential evapotranspiration may be a specific source of hydrologic model-related uncertainty since different hydrologic models employ different methods as well as require different meteorological variables (Thompson et al., 2014). However, ET scheme of H08 model uses Bulk formula where bulk transfer coefficient is used in calculating the turbulent heat fluxes (Haddeland et al., 2011). In estimating potential evapotranspiration (PET) and hence ET, H08 uses humidity, air temperature, wind speed and radiation. Figure 8 presents the correlation of ET with different meteorological variables (precipitation, specific humidity, air temperature and net radiation) for three basins. ET of Brahmaputra shows significant correlation with precipitation, air temperature, specific humidity and net radiation (correlation coefficient (cc) ranges from 0.70 to 0.89) and ET of Meghna also strongly correlated with those meteorological variables (cc ranges from 0.74 to 0.90) except net radiation (cc = 0.45). However, ET of Ganges has weak correlation with those meteorological variables (cc ranges from 0.27 to 0.56). This might be due to upstream water use (which is larger in Ganges) is estimated as ET by current model, which lead to inaccurate estimation of actual ET in this basin and hence weaker correlation of ET with meteorological variables.

4.3 Inter-annual variability

Figure 9 presents inter-annual variability of meteorological and hydrological variables for three basins. Long-term trend of annual variability in precipitation is not pronounced because the inter-annual variability in precipitation is quite large. Some dry years (Brahmaputra: 2021, 2030, 2081, 2090; Ganges: 2022, 2029, 2083, 2093; Meghna:

2017, 2021, 2081, 2093–2097) and some wet year (Brahmaputra: 2022, 2039, 2079, 2082, 2099; Ganges: 2017, 2025, 2035, 2076, 2096; Meghna: 2019, 2029, 2079, 2084) can be discerned in annual precipitation from the figure. A clear increasing trend in air temperature is observed for all three basins though there exist inter-annual variation.

As there is strong correlation between precipitation and runoff (Fig. 8), inter-annual variability of runoff and precipitation are closely similar. There is no clear trend observed for ET in each basin from present to the near future period. However, in the far future a prominent increasing trend is observed for Brahmaputra and Meghna basin (Fig. 9e1 and e3). Though there is no clear trend is noticed for ET of Ganges in far future, inter-annual variation is quite large compared to other two basins. Figure 9f1–f3 plots the annual soil moisture varies from year to year owing to inter-annual variability of the simulated precipitation and evapotranspiration. However, because no clear trend is identifiable in the precipitation and evapotranspiration rates, the effect of climate change on soil moisture is not pronounced.

4.4 Projected changes in the mean

4.4.1 Precipitation

By the end of 21st century; mean precipitation is projected to increase by 14.0, 10.4, and 15.2 % in Brahmaputra, Ganges and Meghna respectively (Table 3). This observation is in agreement with previous studies that compared the performance of GCMs over this region. For example, Immerzeel (2008) measured increases of precipitation in Brahmaputra basin as 22 and 14 % for 2 different scenario. However, Endo et al. (2012) estimated country-wise which are 19.7 and 13 % for Bangladesh and India accordingly. It is observed that changes of precipitation in dry season (November–April) (Brahmaputra: 16 %, Ganges: 23 %, Meghna: 29 %) are larger than that in wet season (May–October) (Brahmaputra: 13.5 %, Ganges: 7.5 %, Meghna: 11 %) (Fig. 11a–c).

Discussion Paper | Discussion Paper | Discussion Paper | Discussion Paper |

HESSD

11, 5747–5791, 2014

4.4.2 Air temperature

The entire GBM basin will be warmer by ~ 1 and ~ 3 °C (Brahmaputra: 3.2 °C, Ganges: 2.9 °C, Meghna: 2.6 °C) in near-future and far-future respectively if the simulated future climate becomes true. According to projected changes, cool basin Brahmaputra will be much warm with maximum increase up to 3.8 °C in February and October (Fig. 11d). In previous literature (Immerzeel, 2008), increase of air temperature in Brahmaputra was projected as 2.3 ~ 3.5 °C by the end of 21st century. However, rate of increse over a season is not uniform for all basins. Temperature will increase more in winter than that in summer (Fig. 11d–f). Therefore, due to seasonal varying rate of increase of air temperature, shorter winter and an extended spring season might be expected in future, which might affect crop growing season as well.

4.4.3 Runoff

Mean runoff is predicted to be increased by about 14, 15, and 18 % in Brahmaputra, Ganges and Meghna respectively (Table 3) by the end of the century. Percentage increase of runoff in Brahmaputra will be large in March, April (about 30 %), which might be due to increase of precipitation as well as higher snow melting caused by large increase of temperature in February (Fig. 11d). In response of seasonal varying rate of changes of air temperature and of precipitation, changes of runoff in dry season (November–April) (Brahmaputra: 15.7 %, Ganges: 18.1 %, Meghna: 27.6 %) are larger than that in wet season (May–October) (Brahmaputra: 13.4 %, Ganges: 14.6 %, Meghna: 15.8 %) (Fig. 11j and k). Runoff of Meghna shows larger response to precipitation. Larger changes of runoff in Meghna directed to higher possibility of flood in this basin which may stipulate the prolong flood in Bangladesh. These findings are consistent with previous findings. Mirza (2002) reported that probability of occurrence of 20 year floods are expected to be higher in Brahmaputra and Meghna rivers than in Ganges rivers. However, Mirza et al. (2003) found future changes in the peak discharge

HESSD
11, 5747–5791, 2014

Impacts of future climate change on the hydrology of GBM basin

M. Masood et al.

of the Ganges (as well as Meghna) river are expected to be larger than those of the Brahmaputra river.

4.4.4 Evapotranspiration

It is observed in Fig. 11m–o, changes of ET in near-future are very less (even 2 % decrease in mean of Meghna). However, by the end of the century increases are quite large (Brahmaputra: 14.4 %, Ganges: 9.4 %, Meghna: 8.8 %) which might be enhanced by the increase of net radiation (Brahmaputra: 6 %, Ganges: 5.9 %, Meghna: 3.3 %) as well as warmer air temperature. In near-future, ET of Meghna is projected to be decreased, which might be due to less change of air temperature (0.7 °C) and decrease of net radiation in this basin. Following the seasonal pattern of radiation (Fig. 11g–i) and air temperature (Fig. 11d–f) changes of ET will be much larger in dry season (November–April) (Brahmaputra: 18.5 %, Ganges: 18.7 %, Meghna: 15.2 %) than that in wet season (May–October) (Brahmaputra: 12.8 %, Ganges: 4.3 %, Meghna: 6.2 %).

4.4.5 Soil moisture

Soil moisture is expressed in terms of water height per unit area within spatially varying soil depths (3 ~ 5 m). Changes of soil moisture (ranges 1 ~ 8.7 % in the far-future) are less (except for Meghna in March–April it is projected to rise up to 30 %) compared to other hydrological quantities. However, the associated uncertainties through all seasons are relatively high (Fig. 10f1–f3).

4.4.6 Net radiation

Fig. 11g–i presents projected changes of net radiation. In the far-future changes of net radiation are larger in dry season (Brahmaputra: 10.5 %, Ganges: 8.8 %, Meghna: 3.9 %) than that in wet season (Brahmaputra: 3.8 %, Ganges: 4.4 %, Meghna: 2.9 %). Due to projected air temperature increase in dry period is large, downward long-wave radiation would be large too, which results larger increase of net radiation in dry

HESSD
11, 5747–5791, 2014

period. In the near-future, changes of net radiation are quite low with 3.1 % decrease in Meghna basin and almost constant through all seasons. Decrease of net radiation of Meghna in near-future might be due to lower increase of air temperature (0.7 °C) as well as decreased incoming solar radiation (not showed in figure) in this basin.

4.5 Uncertainty in projection due to model parameter

In recent decades, along with the increasing computational power there has been a trend towards increasing complex hydrological models to capture natural phenomenon more precisely. However, the increased complexity of hydrological models does not necessarily improve their performance for unobserved conditions due to uncertainty in the values of the model parameters (Carpenter and Georgakakos, 2006; Tripp and Niemann, 2008). An increase in complexity may improve the calibration performance due to the increased flexibility in the model behaviour, but the ability to identify correct parameter values is typically reduced (Wagener et al., 2003). Even it is possible that many parameter sets can reproduce the observations with similar accuracy. Another source of uncertainty comes though assumption of stationary model parameter overtime. This is one of the major limitations of modelling the effect of climate change that model parameters are estimated from the current climate as a basis for predicting future conditions while the behaviour of physical parameters of a catchment is not necessarily stationary overtime (Mirza and Ahmad, 2005b). Therefore, uncertainty of future projection due to model parameter should consider carefully, which is mostly ignored in the climate change impact studies (Lespinas et al., 2014). To assess this uncertainty, in our study, average results from 10 different simulation with considering 10 optimal parameter set according to Nash–Sutcliffe efficiency (NSE) (Nash and Sutcliffe, 1970) have been considered for estimating future changes. This study also identifies which variable is relatively more uncertain to predict and how much uncertain it is.

Figure 10c1–f3 plots seasonal cycle as well as uncertainty band (color shading) of hydrological quantities and net radiation of present-day, near-future and far-future

HESSD
11, 5747–5791, 2014

periods. It is observed that uncertainty band of runoff is relatively narrow, which means runoff is well predictable through hydrologic model simulation. Alternately, it can be said that uncertainty due to non-stationary model parameter in estimation of runoff is less (coefficient of variation (CV) ranges 2–15 % for three basins) compared to that of other hydrologic variable (Fig. 10d1–d3). In addition, from Fig. 5 it is observed that there is no significant uncertainty in simulated peak discharge for Brahmaputra and Meghna river. Lower uncertainty in predicting runoff might be significant for studies, for instance, flood risk assessment where estimation of runoff (especially peck flow) is the main focus and therefore, model parameter-related uncertainty could be ignored. However, relatively wide uncertainty band of runoff has been found for Ganges basin in wet season (Fig. 10d2). While the model can predict runoff well for other two basins, uncertainty in runoff of Ganges might not come from any specific model parameter rather might be due to model setup with ignoring upstream huge water usage in this basin. This uncertainty could be addressed by calibrating the model with considering water usages. However, lower uncertainty in runoff due to model parameter is quite expected as model is calibrated and validated against observed discharge data at basin outlet, which makes model (with optimal parameter set) capable to estimate runoff precisely. In estimating ET, uncertainty is also less (CV ranges 4–20 %), which results less uncertainty of runoff estimation as well. ET of Ganges can be predicted well as it shows narrower uncertainty band in calculating net radiation (CV is 1 %) and subsequently in calculating evapotranspiration (CV is 4 %) (Fig. 10e2). On the other hand, estimation of soil moisture is quite uncertain in all basins (CV ranges 11–33 %). Larger uncertainty in predicting soil moisture is significant in land use management, agriculture in particular and indicates that precise estimation of soil moisture is necessary through physical observation. This finding also highlights the necessity of physical identification of model parameters.

Figure 11 plots future percentage changes of monthly mean of hydrological quantities and net radiation of near-future and far-future period from means of current period. Average results from 10 different simulations are considered to calculate the

Discussion Paper | Discussion Paper | Discussion Paper | Discussion Paper |

HESSD

11, 5747–5791, 2014

Impacts of future climate change on the hydrology of GBM basin

M. Masood et al.

percentage future change. However, if non-stationary parameter is considered, these percentage changes will be different. Table 4 presents standard deviations of mean percentage changes. As expected, for Brahmaputra and Meghna uncertainty in runoff is less; standard deviation of which ranges from 4.2 (4.3) to 14.8 (15.7) in near-future (far-future). However, uncertainty in soil moisture is quite large; standard deviation of which ranges from 21.1 (20.2) to 35.1 (34.8) in near-future (far-future)

5 Conclusion

This study presents model analyses of the climate change impact on Ganges–Brahmaputra–Meghna (GBM) basin focusing on (1) the calibration and validation of the hydrologic model H08 and (2) the impacts of future climate changes in the basin-scale hydrology. The uncertainties in the future projection stemming from model parameter were also assessed. The time-slice numerical experiments were performed using the H08 model forced by the climatic variables from the high-resolution (20 km) climate model (MRI-AGCM3.2S) simulations for the present-day (1979–2003), near-future (2015–2039) and the far-future (2075–2099) periods.

The following findings and conclusions were drawn:

- By the end of 21st century (a) the entire GBM basin is projected to be warmer by ~ 3 °C (Brahmaputra: 3.2 °C, Ganges: 2.9 °C, Meghna: 2.6 °C), (b) the changes of mean precipitation are projected to be +14.0, +10.4, and +15.2 %, and the changes of mean runoff to be +14, +15, and +18 % in the Brahmaputra, Ganges and Meghna basin, respectively (Table 3), (c) evapotranspiration (ET) is predicted to increase significantly for the entire GBM basins (Brahmaputra: 14.4 %, Ganges: 9.4 %, Meghna: 8.8 %), though very less changes in near-future, (d) changes of soil moisture (ranging 1 ~ 8.7 %) are less compared to other hydrological quantities. Larger changes of ET might be due to higher increase of net radiation (Brahmaputra: 6 %, Ganges: 5.9 %, Meghna: 3.3 %) as well as warmer air temperature. Changes of ET will be much larger in dry season (November–April)

HESSD
11, 5747–5791, 2014

(Brahmaputra: 18.5 %, Ganges: 18.7 %, Meghna: 15.2 %) than that in wet season (May–October) (Brahmaputra: 12.8 %, Ganges: 4.3 %, Meghna: 6.2 %). Larger ET in dry season might be due to larger net radiation, air temperature and water availability (increasing precipitation) than that in wet season.

- Over all, it is observed that climate change impact on the hydrology of the Meghna basin is larger than that of the other two basins. For example, in the near-future runoff of Meghna is predicted to increase 11.5 % whereas it is 6 and 2.1 % for Brahmaputra and Ganges respectively. Larger increase of precipitation (15.2 %) in far-future and lower increase of ET (8.8 %) and consequently larger increase of runoff (18 %) lead to higher possibility of flood in this basin. Sea level rise due to climate change will also cause higher floods in this basin as it has tidal influence.

- In estimation of runoff, model parameter-related uncertainty is less, because the model is calibrated against observed discharge data. Besides runoff, uncertainty in estimation of evapotranspiration and net radiation is also relatively less. However, the uncertainty in estimation of soil moisture is quite large (coefficient of variation ranges from 11 to 33 % for three basins). It is significant in land use management, agriculture in particular and indicates the necessity of physical observation of soil moisture. This finding also highlights the necessity of physical identification of model parameters.

However this study still has some limitations which can be addressed in future research; (a) all results presented here are basin-averaged. The basin-averaged large scale changes and trends are difficult to translate to regional and local scale impacts. Moreover, the changes in averages do not reflect the changes in variability and extremes, (b) anthropogenic and industrial water use in upstream are important factors in altering hydrologic cycle, however, which are not considered in present study due to data constraint, (c) only one GCM is used for future climate projection, therefore, the uncertainty due to GCMs are not taken into account in this study, (d) urbanizing watersheds are characterized by rapid land use changes and associated land-scape

HESSD
11, 5747–5791, 2014

disturbances can shift the rainfall–runoff relationships away from natural processes. Hydrological changes in future can also be amplified by changing land uses. However, in our study future changes of demography and land uses are not considered.

Acknowledgements. This study is supported by Public Works Research Institute (PWRI), Japan. The first author is indebted to the authority of Nippon Koei Co., Ltd, Japan for the grant from "The Kubota Fund". Also, thanks are given to A. Hasegawa and T. Sayama for their help in data preparation and for suggestions, and to FFWC, BWDB for providing observed hydrological data.

References

Biemans, H., Speelman, L. H., Ludwig, F., Moors, E. J., Wiltshire, A. J., Kumar, P., Gerten, D., and Kabat, P.: Future water resources for food production in five South Asian river basins and potential for adaptation – a modeling study, Sci. Total Environ., 468–469, Supplement, S117–S131, doi:10.1016/j.scitotenv.2013.05.092, 2013.

Carpenter, T. M. and Georgakakos, K. P.: Intercomparison of lumped vs. distributed hydrologic model ensemble simulations on operational forecast scales, J. Hydrol., 329, 174–185, doi:10.1016/j.jhydrol.2006.02.013, 2006.

Chowdhury, M. R.: An assessment of flood forecasting in Bangladesh: the experience of the 1998 flood, Nat. Hazards, 22, 139–163, 2000.

Chowdhury, M. R. and Ward, M. N.: Hydro-meteorological variability in the greater Ganges–Brahmaputra–Meghna basins, Int. J. Climatol., 24, 1495–1508, doi:10.1002/joc.1076, 2004.

Chowdhury, M. R. and Ward, M. N.: Seasonal flooding in Bangladesh – variability and predictability, Hydrol. Process., 21, 335–347, doi:10.1002/hyp.6236, 2007.

Endo, H., Kitoh, A., Ose, T., Mizuta, R., and Kusunoki, S.: Future changes and uncertainties in Asian precipitation simulated by multiphysics and multi–sea surface temperature ensemble experiments with high-resolution Meteorological Research Institute atmospheric general circulation models (MRI-AGCMs), J. Geophys. Res., 117, D16118, doi:10.1029/2012jd017874, 2012.

FAO-AQUASTAT: Ganges–Brahmaputra–Meghna River Basin, 1, available at: http://www.fao.org/nr/water/aquastat/basins/gbm/index.stm (last access: 19 April 2014), 2014.

Gain, A. K., Immerzeel, W. W., Sperna Weiland, F. C., and Bierkens, M. F. P.: Impact of climate change on the stream flow of the lower Brahmaputra: trends in high and low flows based on discharge-weighted ensemble modelling, Hydrol. Earth Syst. Sci., 15, 1537–1545, doi:10.5194/hess-15-1537-2011, 2011.

Ghosh, S. and Dutta, S.: Impact of climate change on flood characteristics in Brahmaputra basin using a macro-scale distributed hydrological model, J. Earth Syst. Sci., 121, 637–657, doi:10.1007/s12040-012-0181-y, 2012.

Haddeland, I., Clark, D. B., Franssen, W., Ludwig, F., Voß, F., Arnell, N. W., Bertrand, N., Best, M., Folwell, S., Gerten, D., Gomes, S., Gosling, S. N., Hagemann, S., Hanasaki, N., Harding, R., Heinke, J., Kabat, P., Koirala, S., Oki, T., Polcher, J., Stacke, T., Viterbo, P., Weedon, G. P., and Yeh, P.: Multimodel estimate of the global terrestrial water balance: setup and first results, J. Hydrometeorol., 12, 869–884, doi:10.1175/2011jhm1324.1, 2011.

Haddeland, I., Heinke, J., Voß, F., Eisner, S., Chen, C., Hagemann, S., and Ludwig, F.: Effects of climate model radiation, humidity and wind estimates on hydrological simulations, Hydrol. Earth Syst. Sci., 16, 305–318, doi:10.5194/hess-16-305-2012, 2012.

Hanasaki, N., Kanae, S., Oki, T., Masuda, K., Motoya, K., Shirakawa, N., Shen, Y., and Tanaka, K.: An integrated model for the assessment of global water resources – Part 1: Model description and input meteorological forcing, Hydrol. Earth Syst. Sci., 12, 1007–1025, doi:10.5194/hess-12-1007-2008, 2008.

Hanasaki, N., Saito, Y., Chaiyasaen, C., Champathong, A., Ekkawatpanit, C., Saphaokham, S., Sukhapunnaphan, T., Sumdin, S., and Thongduang, J.: A quasi-real-time hydrological simulation of the Chao Phraya River using meteorological data from the Thai Meteorological Department Automatic Weather Stations, HRL – Hydrological Research Letters, 8, 9–14, doi:10.3178/hrl.8.9, 2014.

Hydrological data and maps based on SHuttle Elevation Derivatives at multiple Scales, available at: http://hydrosheds.cr.usgs.gov/hydro.php(last access: 19 April 2014), 2014.

Immerzeel, W.: Historical trends and future predictions of climate variability in the Brahmaputra basin, Int. J. Climatol., 28, 243–254, doi:10.1002/joc.1528, 2008.

Inomata, H., Takeuchi, K., and Fukami, K.: Development of a statistical bias correction method for daily precipitation data of GCM20, Journal of Japan Society of Civil Engineers, 67, I_247–I_252, doi:10.2208/jscejhe.67.I_247, 2011.

Islam, A. S., Haque, A., and Bala, S. K.: Hydrologic characteristics of floods in Ganges–Brahmaputra–Meghna (GBM) delta, Nat. Hazards, 54, 797–811, 2010.

HESSD

11, 5747–5791, 2014

Impacts of future climate change on the hydrology of GBM basin

M. Masood et al.

IWM: Updating and Validation of North West Region Model (NWRM), Institute of Water Modelling, Bangladesh, 2006.
Kamal-Heikman, S., Derry, L. A., Stedinger, J. R., and Duncan, C. C.: A Simple Predictive Tool for Lower Brahmaputra River Basin Monsoon Flooding, Earth Interact., 11, 1–11, doi:10.1175/ei226.1, 2007.
Kamal, R., Matin, M. A., and Nasreen, S.: Response of river flow regime to various climate change scenarios in Ganges–Brahmaputra–Meghna Basin, Journal of Water Resources and Ocean Science, 2, 15–24, doi:10.11648/j.wros.20130202.12, 2013.
Kwak, Y., Takeuchi, K., Fukami, K., and Magome, J.: A new approach to flood risk assessment in Asia-Pacific region based on MRI-AGCM outputs, HRL – Hydrological Research Letters, 6, 70–75, doi:10.3178/HRL.6.70, 2012.
Lehner, B., Verdin, K., and Jarvis, A.: HydroSHEDS technical documentation v1.0, World Wildlife Fund US, Washington, DC, 1–27, 2006.
Lespinas, F., Ludwig, W., and Heussner, S.: Hydrological and climatic uncertainties associated with modeling the impact of climate change on water resources of small Mediterranean coastal rivers, J. Hydrol., 511, 403–422, doi:10.1016/j.jhydrol.2014.01.033, 2014.
Lucas-Picher, P., Christensen, J. H., Saeed, F., Kumar, P., Asharaf, S., Ahrens, B., Wiltshire, A. J., Jacob, D., and Hagemann, S.: Can Regional Climate Models Represent the Indian Monsoon?, J. Hydrometeorol., 12, 849–868, doi:10.1175/2011jhm1327.1, 2011.
Manabe, S.: Climate and the ocean circulation – 1: The atmospheric circulation and the hydrology of the Earth's surface, Mon. Weather Rev., 97, 739–774, 1969.
Mirza, M. M. Q.: Global warming and changes in the probability ofoccurrence of floods in Bangladesh and implications, Global Environ. Chang., 12, 127–138, 2002.
Mirza, M. M. Q.: Three recent extreme floods in Bangladesh: a hydro-meteorological analysis, Nat. Hazards, 28, 35–64, doi:10.1023/A:1021169731325, 2003.
Mirza, M. M. Q. and Ahmad, Q. K. (Eds.): Climate Change And Water Resources in South Asia, A. A. Balkema Publishers, Leiden, Netherlands, 2005.
Mirza, M. M. Q., Warrick, R. A., Ericksen, N. J., and Kenny, G. J.: Trends and persistence in precipitation in the Ganges, Brahmaputra and Meghna River Basins, Hydrolog. Sci. J., 43, 345–858, 1998.
Mirza, M. M. Q., Warrick, R. A., and Ericksen, N. J.: The implications of climate change on floods of the Ganges, Brahmaputra and Meghna rivers in Bangladesh, Climatic Change, 57, 287–318, 2003.

HESSD
11, 5747–5791, 2014

Impacts of future climate change on the hydrology of GBM basin

M. Masood et al.

Mizuta, R., Yoshimura, H., Murakami, H., Matsueda, M., Endo, H., Ose, T., Kamiguchi, K., Hosaka, M., Sugi, M., Yukimoto, S., Kusunoki, S., and Kitoh, A.: Climate Simulations Using MRI-AGCM3.2 with 20 km Grid, J. Meteorol. Soc. Jpn., 90, 233–258, doi:10.2151/jmsj.2012-A12, 2012.

Nash, J. E. and Sutcliffe, J. V.: River flow forecasting through conceptual models Part I – A discussion of principles, J. Hydrol., 10, 282–290, 1970.

NEO: Normalized Difference Vegetation Index [NDVI] (1 Month – Terra/Modis), available at: http://neo.sci.gsfc.nasa.gov/view.php?datasetId=MOD13A2_M_NDVI&year=2000 (last access: 19 April 2014), 2014.

Nishat, A. and Faisal, I. M.: An Assessment of the Institutional Mechanism for Water Negotiations in the Ganges–Brahmaputra–Meghna system, International Negotiations, 5, 289–310, doi:10.1163/15718060020848776, 2000.

Nishat, B. and Rahman, S. M. M.: Water resources modeling of the Ganges–Brahmaputra–Meghna River Basins using satellite remote sensing data, JAWRA J. Am. Water Resour. As., 45, 1313–1327, doi:10.1111/j.1752-1688.2009.00374.x, 2009.

Oki, T. and Sud, Y. C.: Design of Total Runoff Integrating Pathways (TRIP) – a global river channel network, Earth Interact., 2, 1–37, 1998.

Pfly: Ganges-Brahmaputra-Meghna basins.jpg, available at: http://en.wikipedia.org/wiki/File:Ganges-Brahmaputra-Meghna_basins.jpg, last access: April 2014, 2011.

Pokhrel, Y., Hanasaki, N., Koirala, S., Cho, J., Yeh, P. J. F., Kim, H., Kanae, S., and Oki, T.: Incorporating anthropogenic water regulation modules into a land surface model, J. Hydrometeorol., 13, 255–269, doi:10.1175/jhm-d-11-013.1, 2012.

Rahman, M. M., Ferdousi, N., Sato, Y., Kusunoki, S., and Kitoh, A.: Rainfall and temperature scenario for Bangladesh using 20 km mesh AGCM, International Journal of Climate Change Strategies and Management, 4, 66–80, doi:10.1108/17568691211200227, 2012.

Sevat, E. and Dezetter, A.: Selection of calibration objective functions in the context of rainfall–runoff modeling in a Sudanese savannah area, Hydrolog. Sci. J., 36, 307–330, 1991.

Shaaban, A. J., Amin, M. Z. M., Chen, Z. Q., and Ohara, N.: Regional modeling of climate change impact on peninsular Malaysia water resources, J. Hydrol. Eng., 16, 1040–1049, doi:10.1061/(ASCE)HE.1943-5584.0000305, 2011.

Siderius, C., Biemans, H., Wiltshire, A., Rao, S., Franssen, W. H., Kumar, P., Gosain, A. K., van Vliet, M. T., and Collins, D. N.: Snowmelt contributions to discharge of the Ganges, Sci. Total Environ., 468–469 Suppl, S93-S101, doi:10.1016/j.scitotenv.2013.05.084, 2013.

Thompson, J. R., Green, A. J., and Kingston, D. G.: Potential evapotranspiration-related uncertainty in climate change impacts on river flow: an assessment for the Mekong River basin, J. Hydrol., 510, 259–279, doi:10.1016/j.jhydrol.2013.12.010, 2014.
Tripp, D. R. and Niemann, J. D.: Evaluating the parameter identifiability and structural validity of a probability-distributed model for soil moisture, J. Hydrol., 353, 93–108, doi:10.1016/j.jhydrol.2008.01.028, 2008.
Wagener, T., McIntyre, N., Lees, M. J., Wheater, H. S., and Gupta, H. V.: Towards reduced uncertainty in conceptual rainfall–runoff modelling: dynamic identifiability analysis, Hydrol. Process., 17, 455–476, doi:10.1002/hyp.1135, 2003.
Weedon, G. P., Gomes, S., Viterbo, P., Österle, H., Adam, J. C., Bellouin, N., Boucher, O., and Best, M.: The watch forcing data 1958–2001: a meteorological forcing dataset for land surface- and hydrological-models, WATCH Technical Report No. 22, 1–41, 2010.
Weedon, G. P., Gomes, S., Viterbo, P., Shuttleworth, J., Blyth, E., Osterle, H., Adam, J. C., Bellouin, N., Boucher, O., and Best, M.: Creation of the WATCH forcing data and its use to assess global and regional reference crop evaporation over land during the twentieth century, J. Hydrometeorol., 12, 823–848, doi:10.1175/2011JHM1369.1, 2011.
Yatagai, A., Kamiguchi, K., Arakawa, O., Hamada, A., Yasutomi, N., and Kitoh, A.: APHRODITE: constructing a long-term daily gridded precipitation dataset for Asia based on a dense network of rain gauges, B. Am. Meteorol. Soc., 93, 1401–1415, doi:10.1175/BAMS-D-11-00122.1, 2012.

Table 1. Basic input data used in this study.

Type	Description	Source/Reference(s)	Original spatial resolution	Period	Remarks
Physical data	Digital Elevation Map (DEM)	HydroSHEDS[a] (HydroSHEDS, 2014)	15″ (∼ 0.5 km)	–	Global data
	Basin mask	HydroSHEDS[a] (HydroSHEDS, 2014)	30″ (∼ 1 km)	–	
Meteorological data	Rainfall, snowfall, surface pressure, air temperature, specific humidity, wind speed, long-wave downward radiation, shortwave downward radiation	WFD[b] (Weedon et al., 2010; Weedon et al., 2011)	0.5°	1980–2001	5′ (∼ 10 km-mesh) data has been prepared by linear interpolating for this study
	albedo	GSWP2[c]	1°	1980–1990	Mean monthly 5′ (∼ 10 km-mesh) data has been prepared for this study
Hydrologic data	Water level discharge	Bangladesh Water Development Board (BWDB)	Gauged	1980–2012	water level (daily), discharge (weekly) data at outlets of three basins, i.e. the Ganges basin at Hardinge Bridge, the Brahmaputra basin at Bahadurabad, and the Meghna basin at Bhairab Bazar obtained from BWDB.
AGCM data	Rainfall, snowfall, surface pressure, air temperature, specific humidity, wind speed, long-wave downward radiation, shortwave downward radiation	MRI-AGCM3.2S[d] (Mizuta et al., 2012)	0.25° (∼ 20 km-mesh)	1979–2003, 2015–2039, 2075–2099	bias of precipitation dataset has been corrected by multiplying a correction coefficient (ratio between basin averaged long term yearly mean precipitation from WFD and that from MRI) for each GBM basins

[a]HydroSHEDS is Hydrological data and maps based on SHuttle Elevation Derivatives at multiple Scales,
[b]WFD is WATCH forcing data,
[c]GSWP2 is Second Global Soil Wetness Project,
[d]MRI-AGCM is Meteorological Research Institute-Atmospheric General Circulation Model.

HESSD
11, 5747–5791, 2014

Table 2. The 22 year (1980–2001) mean meteorological (WFD forcing dataset) and hydrological variables in the GBM river basins.

	Unit	Brahmaputra	Ganges	Meghna
1. Meteorological variables				
Precipitation (Prcp)	mm year^{-1}	1609	1157	3212
Temperature (Tair)	$^{\circ}$C	9.1	21.7	23.0
Net radiation (Net rad)	W m^{-2}	30	74	78
Specific humidity	g kg^{-1}	9.3	11.8	14.4
2. Hydrological variables				
Runoff	mm year^{-1}	1365	387	2504
Evapotranspiration (ET)	mm year^{-1}	252	774	701
Potential Evapotranspiration (PET)	mm year^{-1}	416	2358	1705

HESSD
11, 5747–5791, 2014

Table 3. 10-simulation average of annual mean and percentage changes of hydrological and meteorological variables.

Variable	Period	Brahmaputra annual mean	Brahmaputra % change (Tair: °C) dry season (Nov–Apr)	Brahmaputra % change (Tair: °C) wet season (May–Oct)	Brahmaputra % change (Tair: °C) annual	Ganges annual mean	Ganges % change (Tair: °C) dry season (Nov–Apr)	Ganges % change (Tair: °C) wet season (May–Oct)	Ganges % change (Tair: °C) annual	Meghna annual mean	Meghna % change (Tair: °C) dry season (Nov–Apr)	Meghna % change (Tair: °C) wet season (May–Oct)	Meghna % change (Tair: °C) annual
(a) Meteorological variables													
Pricipitation	present-day (1979–2003)	1736	–	–	–	1187	–	–	–	3174	–	–	–
(mm year^{-1})	near-future (2015–2039)	1830	2.5	6.3	5.5	1201	10.7	–.9	1.2	3415	5.9	8.1	7.6
	far-future (2075–2099)	1980	16.0	13.5	14.0	1309	23.1	7.5	10.4	3656	29.5	11.2	15.2
Tair	present-day (1979–2003)	5.6	–	–	–	21.2	–	–	–	22.8	–	–	–
(°C)	near-future (2015–2039)	6.6	1.1	1.0	1.0	22.2	0.9	1.1	1.0	23.5	0.7	0.7	0.7
	far-future (2075–2099)	8.8	3.4	3.1	3.2	24.1	2.9	2.9	2.9	25.4	2.9	2.4	2.6
Net radiation	present-day (1979–2003)	64	–	–	–	101	–	–	–	110	–	–	–
(W m^{-2})	near-future (2015–2039)	64	2.0	0.1	0.7	101	1.8	–.4	0.4	106	−3.1	−3.1	−3.1
	far-future (2075–2099)	68	10.5	3.8	6.0	107	8.8	4.4	5.9	113	3.9	2.9	3.3
(b) Hydrological variables													
Total runoff	present-day (1979–2003)	1277	–	–	–	225	–	–	–	2206	–	–	–
(mm year^{-1})	near-future (2015–2039)	1353	4.1	6.5	6.0	230	8.6	1.4	2.1	2459	10.8	11.6	11.5
	far-future (2075–2099)	1455	15.7	13.4	13.9	258	18.1	14.6	14.9	2600	27.6	15.8	17.9
ET	present-day (1979–2003)	460	–	–	–	963	–	–	–	969	–	–	–
(mm year^{-1})	near-future (2015–2039)	477	6.7	2.7	3.8	970	6.1	−2.2	0.7	950	0.4	−2.9	−2.0
	far-future (2075–2099)	526	18.5	12.8	14.4	1053	18.7	4.3	9.4	1054	15.2	6.2	8.8
Soil moisture	present-day (1979–2003)	258	–	–	–	177	–	–	–	323	–	–	–
(mm)	near-future (2015–2039)	260	1.9	0.1	0.8	175	5.7	−4.3	−1.5	337	9.0	2.8	4.4
	far-future (2075–2099)	260	2.5	0.1	1.0	183	11.0	–.2	2.9	351	21.0	4.4	8.7

HESSD

11, 5747–5791, 2014

Impacts of future climate change on the hydrology of GBM basin

M. Masood et al.

Table 4. Statistical indices of uncertainty due to model parameter.

Variable	Period	Brahmaputra		Ganges		Meghna	
		Coefficient variation (CV) of mean (Fig. 10) (%)	Standard deviation of mean percentage change (Fig. 11)	Coefficient variation (CV) of mean (Fig. 10) (%)	Standard deviation of mean percentage change (Fig. 11)	Coefficient variation (CV) of mean (Fig. 10) (%)	Standard deviation of mean percentage change (Fig. 11)
Net radiation	present-day	9	–	1	–	10	–
	near-future	9	9.0	1	1.1	10	10.5
	far-future	8	9.3	1	1.1	10	10.8
Total runoff	present-day	2	–	15	–	9	–
	near-future	2	4.2	15	26.3	7	14.8
	far-future	2	4.3	14	28.8	7	15.7
ET	present-day	7	–	4	–	20	–
	near-future	7	8.0	4	6.2	19	24.6
	far-future	7	8.8	3	6.5	18	25.8
Soil moisture	present-day	33	–	27	–	11	–
	near-future	33	35.1	27	33.7	12	21.1
	far-future	33	34.8	26	34.4	11	20.2

HESSD
11, 5747–5791, 2014

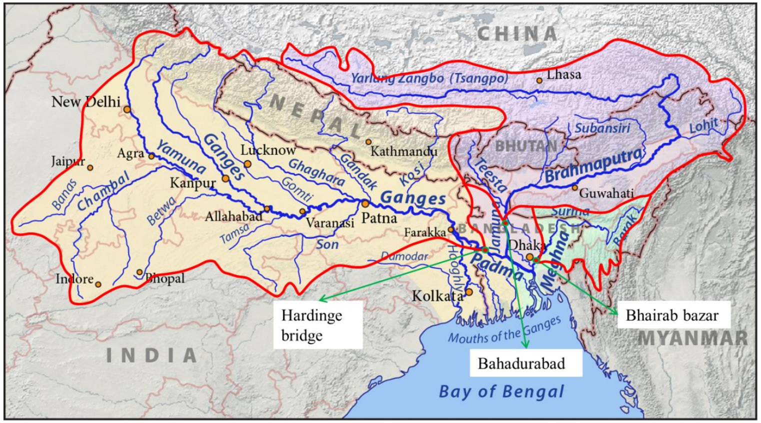

Figure 1. Ganges–Brahmaputra–Meghna (GBM) river basin boundaries (thick red line), upstream of three outlets (green circle); Hardinge bridge, Bahadurabad, and Bhairab bazar respectively (image modified from Pfly, 2011).

HESSD
11, 5747–5791, 2014

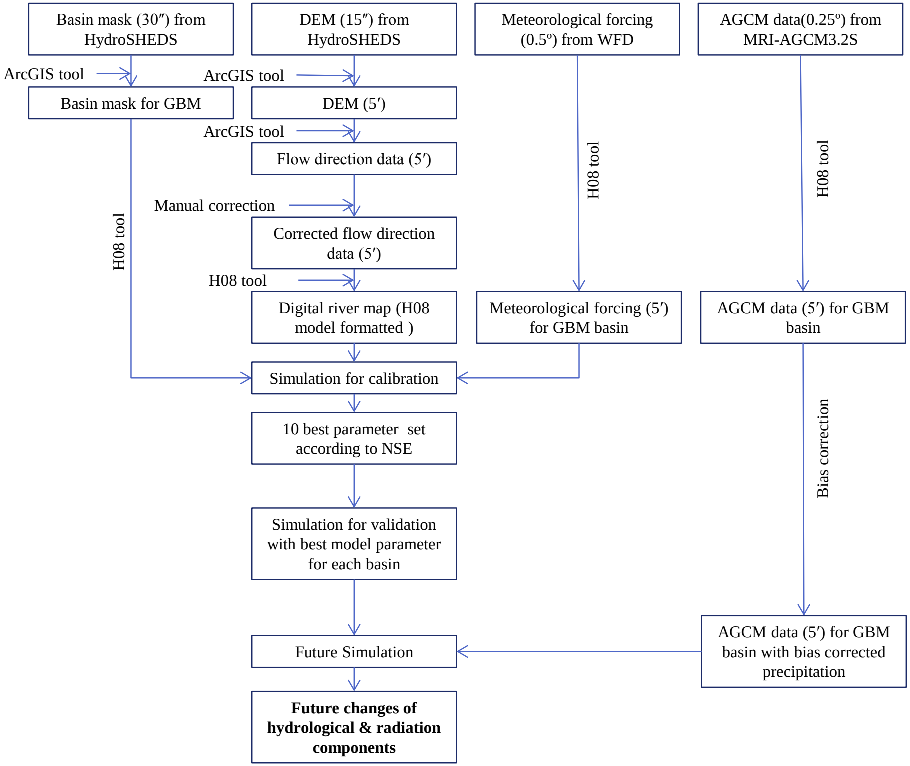

Figure 2. Flow chart of methodology.

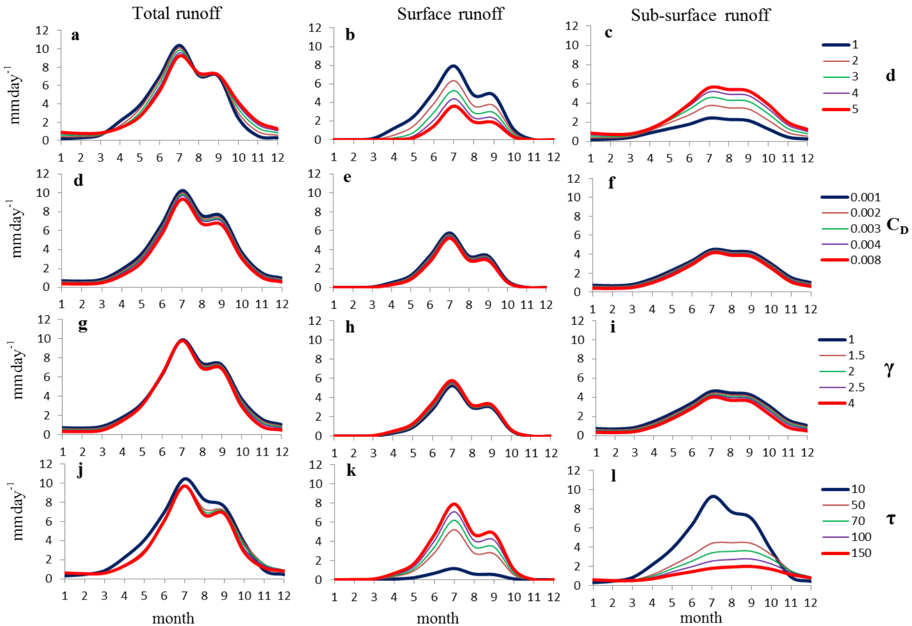

Figure 3. The 11 year (1980–1990) climatology of the simulated total runoff, surface runoff and sub-surface runoff (unit: mm day^{-1}) of Brahmaputra basin. Each of the five lines in each panel represents the average of 5^3 (= 125) runs with one of the four calibration parameters fixed at the given value.

HESSD
11, 5747–5791, 2014

Impacts of future climate change on the hydrology of GBM basin

M. Masood et al.

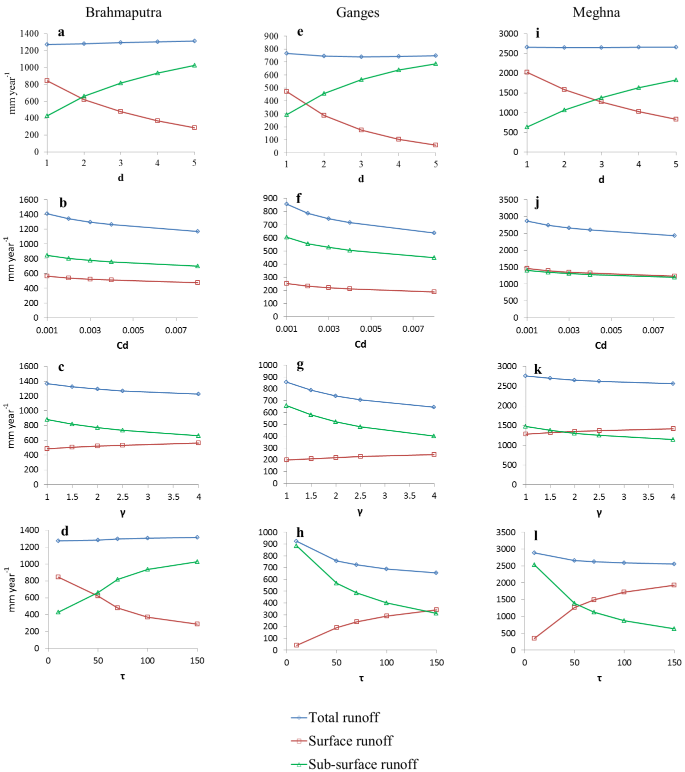

Figure 4. The average annual amounts (unit: mm year^{-1}) of total runoff, surface runoff and sub-surface runoff. Each curve represents the average from the 125 runs with only one of the four parameters (d, C_D, γ, and τ) fixed.

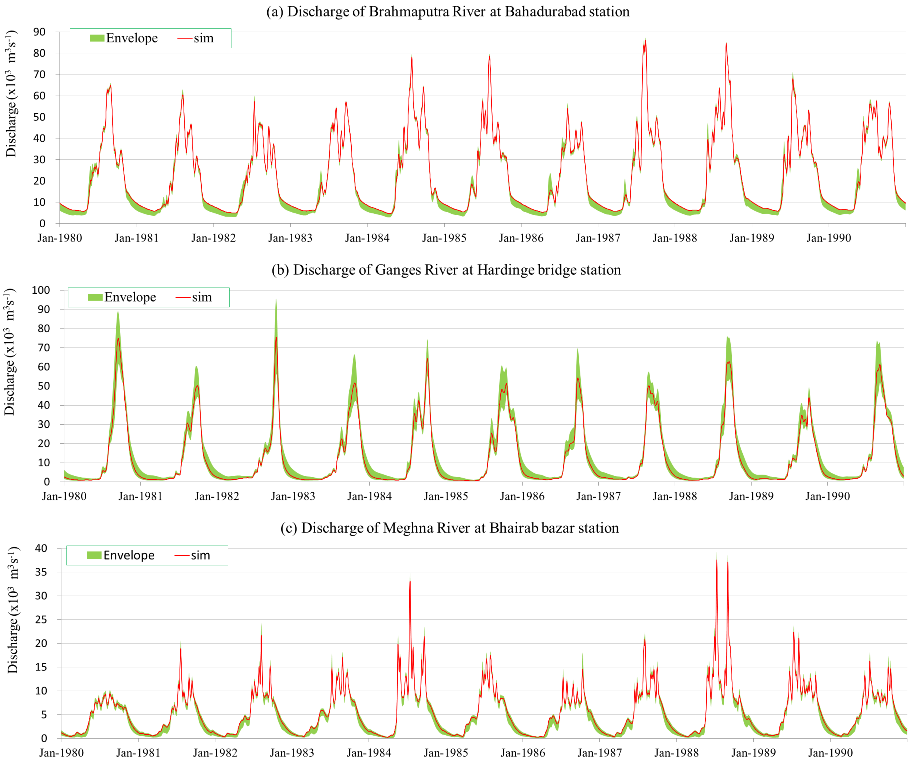

Figure 5. Hydrograph of simulated discharge with optimal parameter set (red line) and envelope of simulated discharge with top 10 optimal parameter combinations (green shading) during calibration period (1980–1990).

HESSD
11, 5747–5791, 2014

Impacts of future climate change on the hydrology of GBM basin

M. Masood et al.

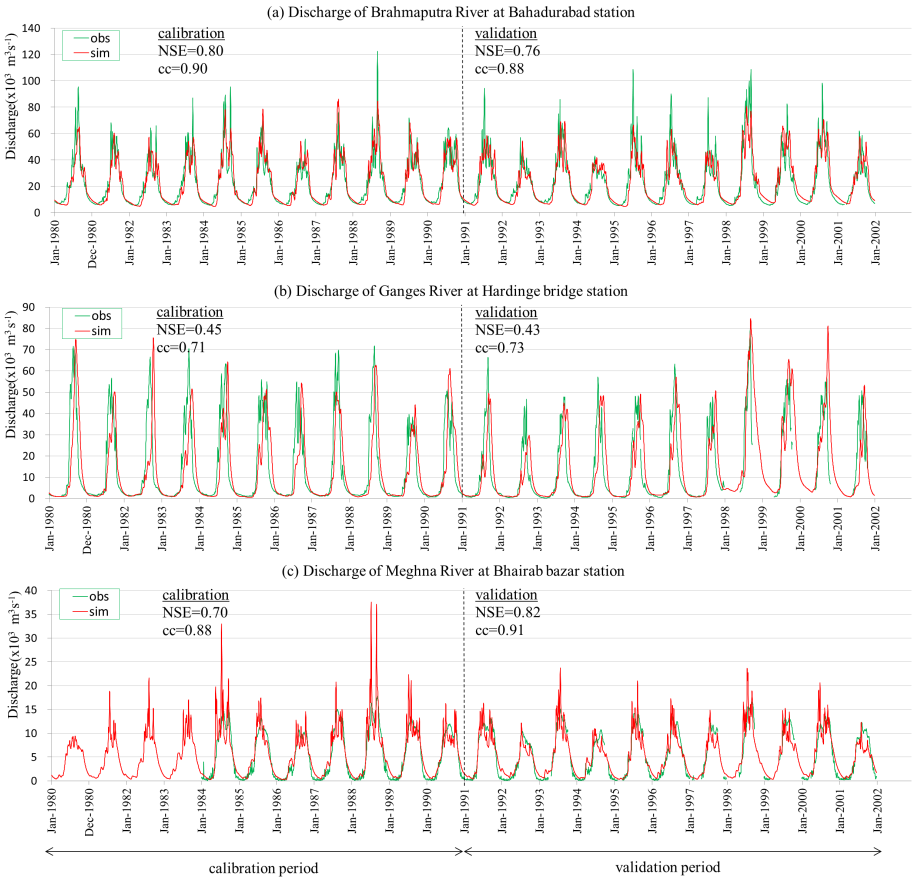

Figure 6. (a–c) Hydrographs (both calibration and validation period) at outlet of three basins. Nash–Sutcliffe efficiency (NSE) and correlation coefficient (cc) for both calibration and validation period are noted at each sub-plot.

HESSD
11, 5747–5791, 2014

Title Page
Abstract
Introduction
Conclusions
References
Tables
Figures
◀
▶
Back
Close
Full Screen / Esc
Printer-friendly Version
Interactive Discussion

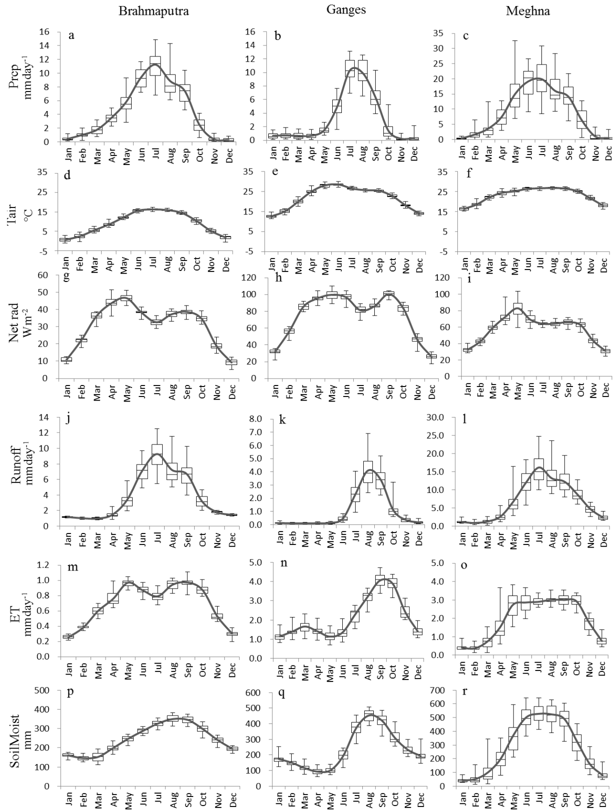

Figure 7. (a–r) Seasonal cycle of climatic and hydrologic quantities during 1980–2001. Box-and-whisker plots indicate minimum and maximum (whiskers), 25th and 75th percentiles (box ends), and median (black solid middle bar). Solid curve line represents inter-annual average value. All abbreviated terms here refer to Table 2.

HESSD
11, 5747–5791, 2014

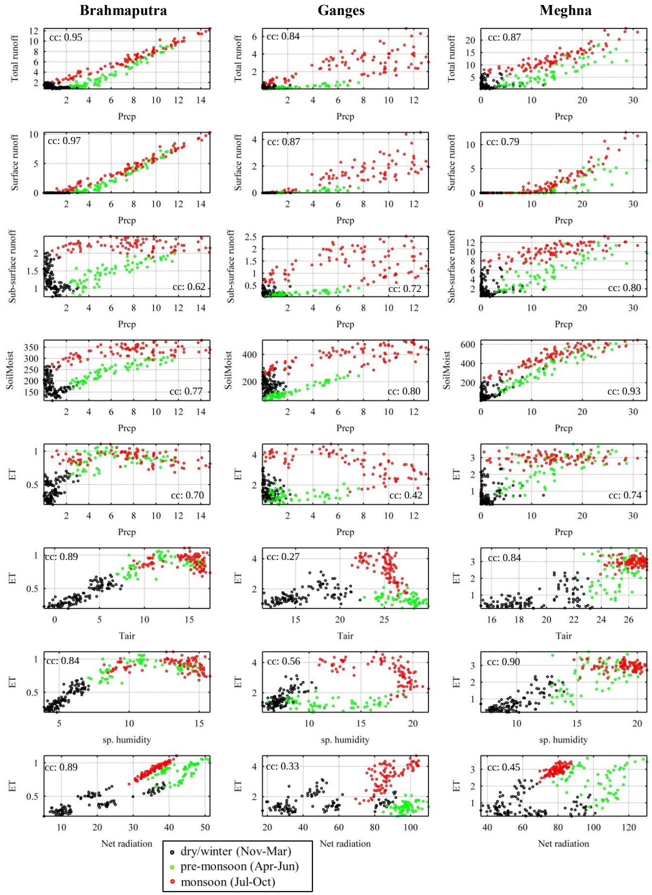

Figure 8. Correlation between monthly mean of meteorological variables (WFD) and that of hydrological variables for Brahmaputra, Ganges and Meghna. Three different color representing data of three different seasons; black: dry/winter (November–March), green: pre-monsoon (April–June) and red: monsoon (July–October). Correlation coefficient (cc) for each pair is noted at each sub-plot. Unit, mm day^{-1} for Prec, ET, runoff, mm for SoilMoist, °C for Tair and W m^{-2} for Net radiation. Figure presents distinct relationship in both season-wise and basin-wise

HESSD
11, 5747–5791, 2014

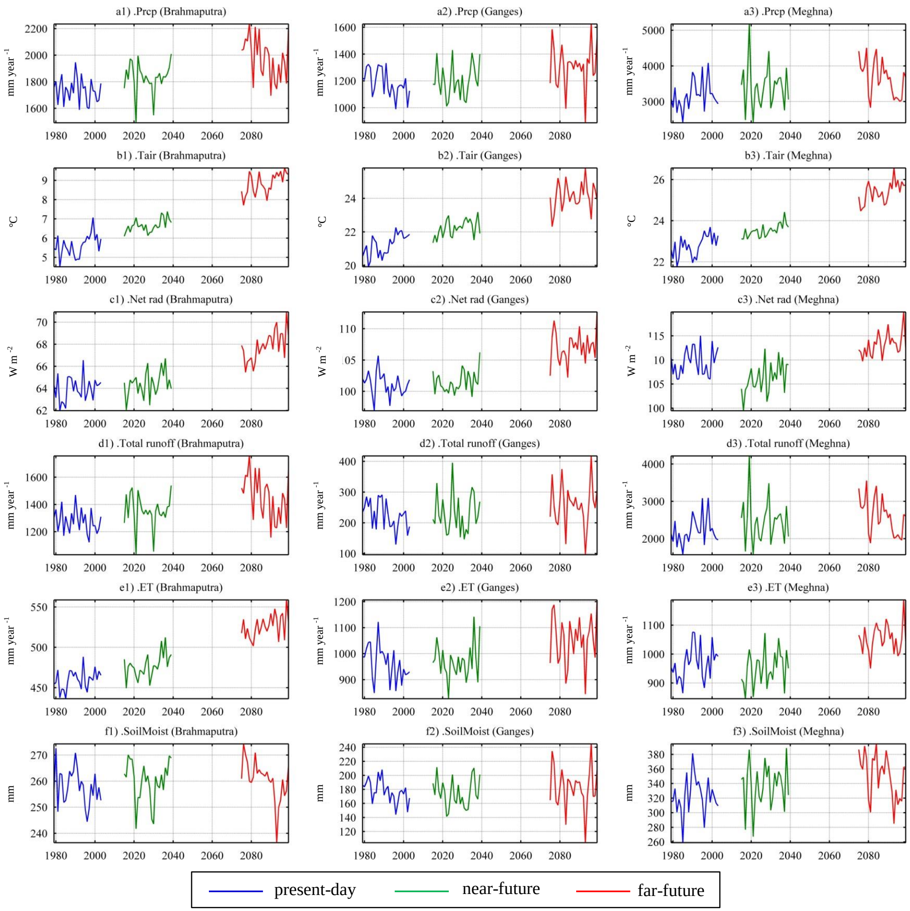

Figure 9. (a1–f3) Inter-annual variation of mean of meteorological and hydrological variables for present-day (blue line), near-future (green line) and far-future (red line).

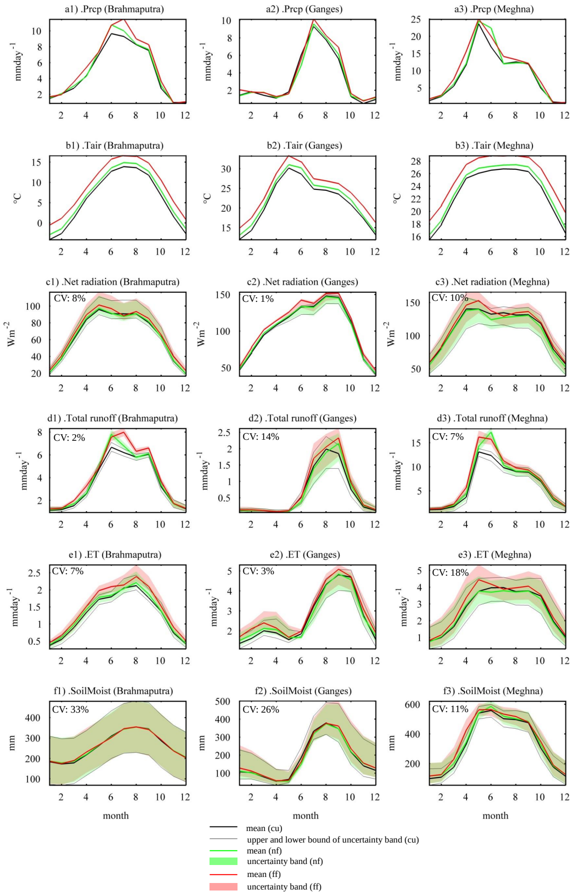

Figure 10. **(a1–f3)** Uncertainty band of hydrological quantities and net radiation components of present-day (grey line), near-future (green shading) and far-future periods (red shading) found from 10 simulation result with considering 10 optimal parameter set according to NSE. Black, green and red solid lines represent mean of 10 simulation results of current, near-future, and far-future respectively (cu: present-day, nf: near-future, ff: far-future). Coefficient of variations (CV) for far-future period (Table 4 presents CV of all periods) are noted at top-left corner in each sub-plot.

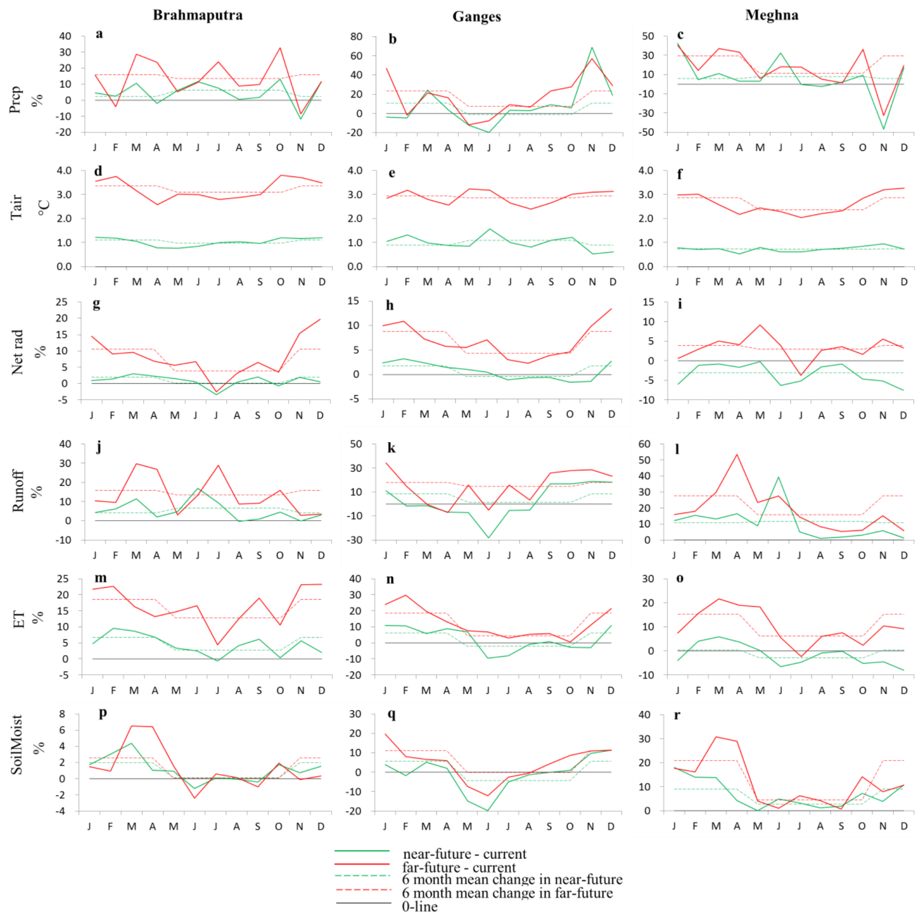

Figure 11. (a–r) Percentage changes of monthly means of climatic and hydrological quantities of near-future and far-future periods from current periods. Dashed lines represent 6 months' mean changes in dry season (November–April) and wet season (May–October).